Low temperature vacuum annealing study of $(Co/Pd)_n$ magnetic multilayers

Chunsheng E, James Rantschler, and Shishan Zhang
Center for Nanomagnetic Systems, University of Houston, Houston, Texas 77204, USA

Sakhrat Khizroev
Electrical Engineering, University of California, Riverside, California 92521, USA

T. Randall Lee and Dmitri Litvinov[a)]
Center for Nanomagnetic Systems, University of Houston, Houston, Texas 77204, USA

(Presented on 9 November 2007; received 11 September 2007; accepted 24 October 2007; published online 4 February 2008)

The correlation between the magnetic properties and the microstructural and chemical composition modifications of Co/Pd magnetic multilayers upon annealing in ultrahigh vacuum at 250 °C is presented. Magnetic characterization using magnetic sample magnetometer shows the vertical magnetic anisotropy increase and the switching field distribution decrease in the annealed samples. The larger values of magnetic anisotropy in the annealed samples are further shown using the magnetic force microscopy of the ac demagnetized states in the Co/Pd multilayer films. X-ray diffraction rocking curves show an improvement in the texture and the initial magnetization curve slopes indicate the decreases in defect densities. Overall, vacuum annealing under optimal conditions improves the magnetic properties of Co/Pd multilayers for applications in ultrahigh density magnetic recording. © *2008 American Institute of Physics*. [DOI: 10.1063/1.2832438]

$(Co/Pd)_n$ magnetic multilayers exhibit high values of perpendicular magnetic anisotropy and are of interest for applications in perpendicular recording and bit-patterned medium recording.[1–4] Perpendicular magnetic anisotropy in these multilayers results from the hybridization of 3*d* and 4*d* electrons of Co and Pd, respectively, at the Co/Pd interfaces and is highly dependent on the interface quality.[5] In multilayers prepared by magnetron sputtering, one of the most common magnetic thin-film synthesis approaches utilized in industrial applications, a certain degree of intermixing at Co/Pd interfaces is expected. The intermixing at the Co/Pd interfaces reduces the perpendicular magnetic anisotropy and its minimization is usually attempted by optimization of the deposition conditions. In this work, we investigated post-deposition thermal annealing as a means to further mitigate the effects of the intermixing at the Co/Pd interfaces instead. It should be noted that while thermal annealing increases the mobility of the atoms near the interfaces and may help promote higher quality interfaces, it can also lead to the diffusion across the interfaces, thus increasing the intermixing.[6]

$(Co/Pd)_n$ multilayer stacks were deposited by magnetron sputtering in an ultrahigh vacuum system with a base pressure of 5×10^{-9} Torr. Deposition was performed at a 2.5×10^{-3} Torr argon pressure at a room temperature on silicon wafers coated with a 0.5 μm thermal oxide. A 20 nm Ta seed layer was used to promote enhanced intergranular exchange coupling,[4] on top of which 30 successive Co(4 Å)/Pd(11 Å) bilayers were deposited. As synthesized multilayers were vacuum annealed at 250 °C in a Philips 5700 x-ray photoelectron spectrometer (XPS) with a base pressure of 10^{-9} Torr. XPS spectra were taken following the annealing to confirm the effects of annealing on chemical composition. XPS spectra revealed the naturally formed CoO_x,[7] whereas oxide peaks (Co_2O_3, Co_3O_4) reported in atmosphere annealed samples were absent.[4] Upon annealing, the intensity ratio of CoO_x to Co $2p_{3/2}$ stayed relatively constant, indicating the absence of oxide growth. X-ray diffraction (XRD) was used to determine the crystal structure, to measure texture, and to evaluate the stress (via lattice constant measurements) in the films. A polar magneto-optical Kerr effect (MOKE) magnetometer and a vibrating sample magnetometer (VSM) were used for magnetic characterization. Magnetic force microscopy (MFM) was used to characterize the demagnetized states of the samples.

The coercivity H_c and nucleation field H_n are plotted versus annealing time in Fig. 1(a). Both H_c and H_n peak with ~30 min of annealing. The magnetization reversal mechanism in the annealed samples was studied by measuring the angular dependence of remnant coercivities.[8–11] In two phase switching starting with domain nucleation and continuing

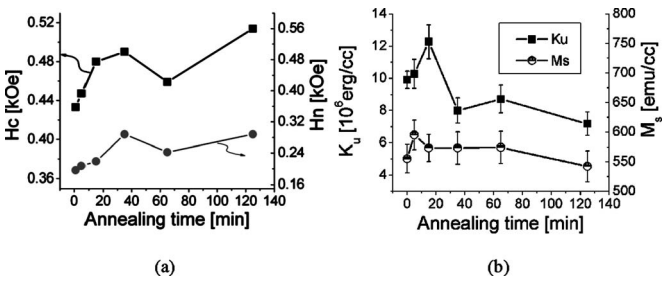

FIG. 1. (a) Coercivity and nucleation field as a function of annealing time. (b) Changes in K_u and M_s as $[Co(4\ Å)/Pd(11\ Å)]_{30}$ was annealed of 250 °C for various durations of time.

[a)]Electronic mail: dlitvinov@uh.edu

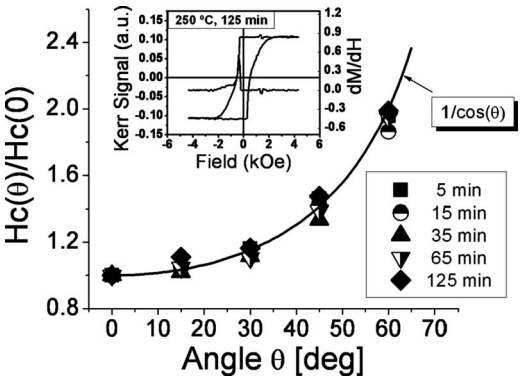

FIG. 2. Angular dependence of the remnant coercivity for $[Co(4\ Å)/Pd(11\ Å)]_{30}$ multilayer annealed for 65 and 125 min. The inset shows the MOKE hysteresis loop and dM/dH curve for the sample annealed for 125 min.

with domain wall motion, the remnant coercivity H_{cr} follows a $1/\cos(\theta)$ relation, where θ is the angle between the applied field and the thin-film normal. The angular dependence of the H_{cr} of the annealed samples is plotted in Fig. 2, and the data points crowd around the $1/\cos(\theta)$ curve. Little difference can be observed among the samples annealed for various durations. In the inset, the hysteresis loop and dM/dH curve for the sample annealed for 125 min are plotted. The hysteresis loop is still characterized by the sharp nucleation edge and the round tail, the same shape as the unannealed sample. It follows that the magnetization switching mechanism is domain nucleation and domain wall motion, independent of the annealing time.

The saturation magnetization M_s was measured by the VSM. The uniaxial anisotropy constant K_u is estimated by measuring the easy and hard axis hysteresis loops and extrapolating to the anisotropy fields [see Fig. 1(b)], resulting in a peak anisotropy of 1.2×10^7 ergs/cm^3 at 15 min and dropping to 8×10^6 ergs/cm^3 thereafter, indirectly indicating optimal surface morphology. A typical MFM image of an ac demagnetized state is illustrated in Fig. 3. The images are subjected to a two-dimensional fast fourier transform and

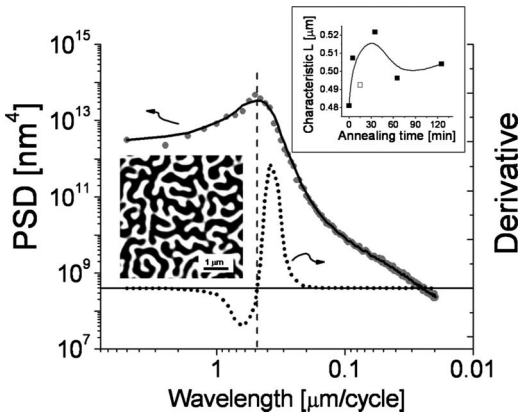

FIG. 3. PSD of the MFM image of ac demagnetized domain state. The dotted line is the derivative curve, whose zero crossing point is considered as the peak position in the PSD and the characteristic length scale of the corresponding domain pattern. The insets shows a $5\times5\ \mu m^2$ scan of the MFM image and the characteristic length scale as a function of annealing time.

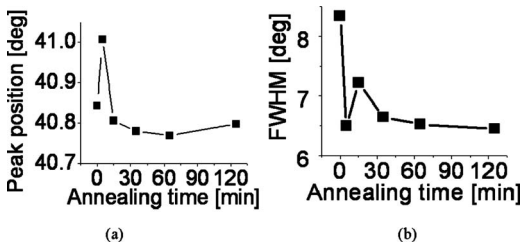

FIG. 4. 111 Pd peak position and (b) FWHM of the (111) rocking curves of $[Co(4\ Å)/Pd(11\ Å)]_{30}$ annealed for (a) 0, (b) 5, (c) 15, (d) 35, (e) 65, and (f) 125 min.

integrated over all the angles in the frequency space. The resulting power density spectrum (PDS) is then differentiated and the zero crossing point of the derivative is taken as the peak position and thus the characteristic length scale of the corresponding domain pattern. The domain wall energy is proportional to $4\sqrt{K_uA}$, where A is the exchange constant of the medium. Since saturation magnetization M_s stays roughly constant, the improvement in perpendicular magnetic anisotropy is confirmed in the widening of the domain patterns observed in the inset. This decreases domain wall density and energy at the cost of increased magnetostatic energy.

XRD analysis showed that as-deposited multilayers have fcc crystal structure and are textured with the (111) direction normal to the plane of the films. The XRD θ-2θ scans near (111) Pd peak and the rocking curves around the same peak are illustrated in Figs. 4(a) and 4(b), respectively. The extracted peak positions and the full width at half maximum (FWHM) are also plotted in the insets. Reduction of the FWHM was observed in all of the annealed samples, indicating the improvements in the texture of the multilayers. The Co lattice spacing along the $(1\bar{1}0)$ direction, the direction in the Co/Pd interfacial plane, is 2.51 Å, whereas the Pd lattice spacing along the $(1\bar{1}0)$ direction is 2.75 Å, which translates into a lattice mismatch of 8.3% at the interfaces. Significantly, the lattice mismatch leads to the defects, which results in magnetic anisotropy inhomogeneities, which, in turn, can provide sites for domain nucleation and/or domain wall pinning.

The samples were then subjected to dc demagnetization (DCD) measurement, in which the irreversible magnetization switching was measured. The derivative of the DCD curve is the irreversible susceptibility at all applied field strengths, whose FWHM is a measure of the SFDs. The switching field distributions (SFDs) of all samples are summarized in Fig. 5.

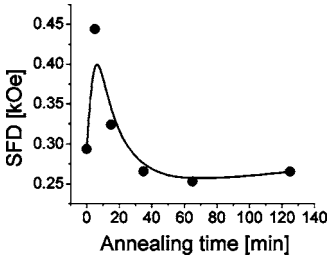

FIG. 5. SFD as a function of annealing time. Improvement in SFD is observed in samples annealed longer than 35 min.

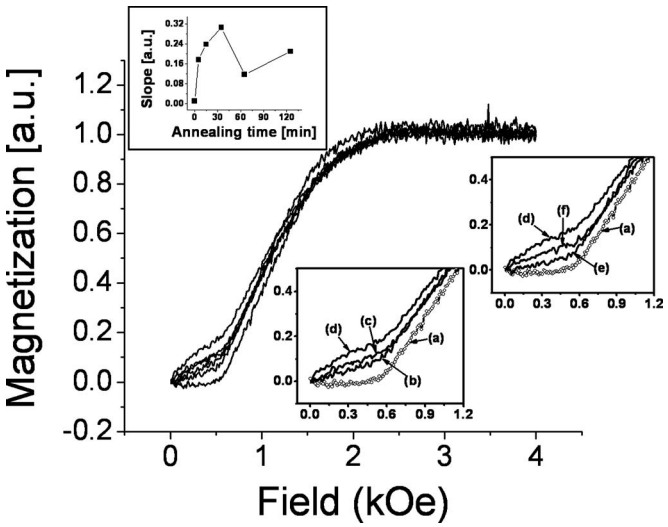

FIG. 6. Initial curves of $[Co(4\ Å)/Pd(11\ Å)]_{30}$ annealed for (a) 0, (b) 5, (c) 15, (d) 35, (e) 65, and (f) 125 min. The insets show in detail the beginning of the initial curves.

As can be seen, annealing improves the SFD for samples annealed longer than 30 min.

To further verify the modification of the microstructure, the samples were ac demagnetized and the initial curves were then measured as shown in Fig. 6. Since the domains have already been nucleated, the initial curve measures how easily the domain walls propagate. We observe that the as prepared sample has the greatest pinning effect. The longer the samples were annealed, the weaker the pinning strength became, indicating a steady decrease in defect densities. Further annealing the sample to 65 and 125 min caused the decrease in the initial susceptibility, as depicted in the second inset of Fig. 6, indicating an increase in defects and confirming the observations in XPS spectra and anisotropy measurements.

In summary, short periods of vacuum annealing lead to higher anisotropy, improved texture spread, lower stress, and greater initial susceptibility and the Pd $3d_{5/2}$ and Co $2p_{3/2}$ peaks in the XPS spectra shift to lower binding energies, indicating sharpening of the interfaces.

This work was supported by the grants from NSF (ECS-0404308, ECS-0421255, ECS-0401297), INSIC, and AFOSR.

[1]D. Weller, A. Moser, L. Folks, M. E. Best, L. Wen, M. F. Toney, M. Schwickert, J. U. Thiele, and M. F. Doerner, IEEE Trans. Magn. **36**, 10 (2000).
[2]C. F. Brucker, J. Appl. Phys. **70**, 6065 (1991).
[3]C. Brucker, T. Nolan, B. Lu, Y. Kubota, M. Plumer, P. L. Lu, R. Cronch, C. H. Chang, D. Chen *et al.*, IEEE Trans. Magn. **39**, 673 (2003).
[4]Ch. E, J. Rantschler, S. Zhang, D. Smith, V. Parekh, S. Khizroev, T. R. Lee, and D. Litvinov, J. Appl. Phys. **101**, 09D108 (2007).
[5]M. Sawada, K. Hayashi, and A. Kakizaki, J. Phys. Soc. Jpn. **72**, 1161 (2003).
[6]F. den Broeder, D. Kuiper, and H. Draaisma, IEEE Trans. Magn. **23**, 3696 (1987).
[7]B. V. Crist, *Handbook of Monochromatic XPS Spectra* (Wiley, New York, 2000).
[8]R. C. Kevin, T. Thomas, and T. Jan-Ulrich, J. Appl. Phys. **92**, 4553 (2002).
[9]T. C. Ulbrich, D. Makarov, G. Hu, I. L. Guhr, D. Suess, T. Schrefl, and M. Albrecht, Phys. Rev. Lett. **96**, 077202 (2006).
[10]M. P. Sharrock and J. T. McKinney, IEEE Trans. Magn. **17**, 3020 (1981).
[11]R. H. Victora, Phys. Rev. Lett. **63**, 457 (1989).